ACS OMEGA

http://pubs.acs.org/journal/acsodf

Article

# Succinonitrile-Polymer Composite Electrolytes for Li-Ion Solid-State Batteries—The Influence of Polymer Additives on Thermomechanical and Electrochemical Properties

Vanessa van Laack, Frederieke Langer, Andreas Hartwig, and Katharina Koschek*

Cite This: *ACS Omega* 2023, 8, 9058−9066

Read Online

ACCESS | Metrics & More | Article Recommendations | Supporting Information

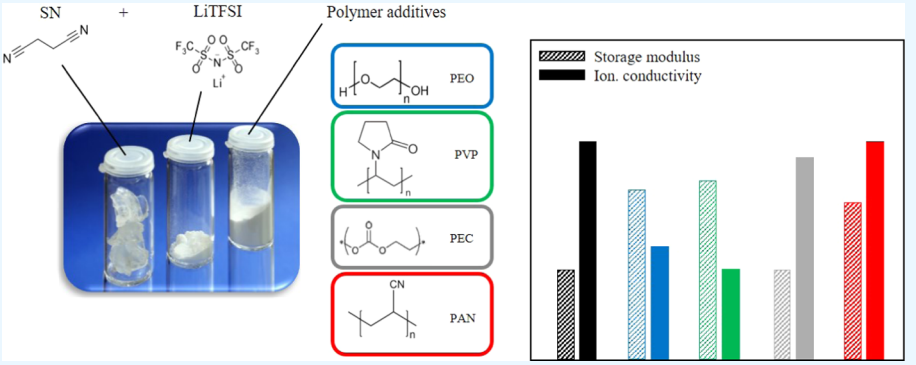


**ABSTRACT:** A plastic crystalline electrolyte (PCE) consisting of 0.4 mol/L lithium bis(trifluoromethanesulfonyl)imide (LiTFSI) in succinonitrile (SN) was blended with poly(ethylene oxide) (PEO), poly(vinylpyrrolidone) (PVP), poly(ethylene carbonate) (PEC), and polyacrylonitrile (PAN). The influences of the regarding polymers on thermomechanical properties of the PCE were studied systematically, utilizing differential scanning calorimetry, thermogravimetric analysis, and oscillation experiments. Depending on the chosen polymer, the melting temperature and overall crystallinity of the PCE were increased. For PCEs containing PEO and PVP, overall crystallinity was enhanced the most resulting in lamellae-like superstructures, identified by light microscopy images. Furthermore, the onset for the sublimation process of SN was shifted to higher temperatures, and the mechanical strength was increased by the presence of some polymers, with exception of PEC. Electrochemical characterization, including electrochemical impedance spectroscopy and linear sweep voltammetry, revealed ionic conductivities of $10^{-4}$ S/cm at room temperature for PCE with PAN and extended electrochemical stability windows of ≥4.5 V vs lithiated graphite for PCE with PEO. By correlating the thermomechanical and electrochemical properties, some structure-property relationships were drawn, pointing out great potential for specific tailoring of PCEs by polymer additives. The synergistic effect of increasing both, mechanical stability and ionic conductivity, made the PCE + PAN composition especially attractive for a possible application in batteries.

## INTRODUCTION

To reach today's criteria for tomorrow's electric devices and to establish e-mobility, the development of feasible battery materials is of high importance. Especially, to enhance safety aspects, durability, performance, and processability, the optimization of an electrolyte has drawn growing interest. Conventional Li-ion batteries (LIBs) contain liquid electrolytes, which limit construction methods and exhibit a risk of leakage and flammability. Therefore, solid electrolyte materials like polymers or ceramics have been widely investigated in various research works[1−7] toward an all-solid-state battery (ASSB). Polymer electrolytes offer advantages with respect to facile processing techniques, low density and therefore, low mass, as well as the possibility of "green" batteries[1] using renewable sources for synthesis. Indeed, other organic compounds being considered for solid-state battery applications that are environmentally friendly are plastic crystals[7,8] like succinonitrile (SN). SN, a derivate of succinic acid, exhibits a plastic crystalline phase from −30 °C until melting at 58 °C.[9,10] Often used as an additive in polymer electrolytes to enhance ionic conductivity,[2,11] SN itself can be applied as a solid electrolyte with an ionic conductivity of up to $10^{-4}$ S/cm at room temperature.[7,12] Although SN exhibits a feasible ionic conductivity, regarding requirements for today's batteries, an SN-based electrolyte suffers from dimensional instability and

**Received:** April 7, 2022
**Accepted:** December 5, 2022
**Published:** March 2, 2023

Table 1. Characteristics of the Selected Polymers

| polymer | $M$, g/mol | morphology | chain length | $N_{polymer}$, mol/g | $N_{RU}$, mol/g |
|---|---|---|---|---|---|
| PEO | 100 000 | semicrystalline | ~2270 | $9.1 \times 10^{-7}$ | $2.1 \times 10^{-3}$ |
| PVP | 25 000 | amorphous | ~225 | $3.6 \times 10^{-6}$ | $8.2 \times 10^{-4}$ |
| PEC | 50 000−200 000 | amorphous | ~568 to 2270 | $1.8 \times 10^{-6}$−$4.6 \times 10^{-7}$ | $1 \times 10^{-3}$ |
| PAN | 80 000 | semicrystalline | ~1508 | $1.1 \times 10^{-6}$ | $1.7 \times 10^{-3}$ |

high sublimation tendency of SN. Further studies demonstrated that through the variation of the molecular structure and concentration of the Li salt or the addition of polymers, material properties like mechanical stability could be improved.[11,13] For example, the addition of polymers like poly(ethylene oxide) (PEO),[14] poly(vinylidenefluoride-*co*-hexafluoropropylene) (PVDF-HFP),[12] or polyacrylonitrile (PAN)[10] enhanced the mechanical properties of SN-based electrolytes, i.e., Young modulus or elongation at break. Additionally, through the solvating qualities of molten SN, a solvent-free integration of polar polymers into the SN-rich electrolyte is possible, and conventional thermal processing methods[13,15] like melt extrusion become accessible. Further, it was demonstrated elsewhere[16] that the addition of PEO to an SN-based electrolyte could decelerate the sublimation of SN, which is favorable to reduce exposition risks during processing. However, the resulting property profile of the SN-based electrolytes with polymers showed a strong dependence on the chosen polymer's molecular structure like functionality or chain length. It is yet to be examined how the thermomechanical properties of an SN-rich electrolyte can be enhanced by the addition of polymers without detrimental effects on electrochemical properties like ionic conductivity.

In this work, the polymers PEO, PVP, PEC, and PAN were selected and their influence on thermomechanical and electrochemical properties of an SN-based electrolyte (0.4 mol/L LiTFSI in SN) was investigated. The polymers varied in their functionality (either carbonyl or nitrile groups) and in their morphology, with PEO and PAN representing semicrystalline polymers and PVP and PEC amorphous polymers. Keeping the "green battery" aspect of SN, the polymers were chosen by their solubility in molten SN, realizing a solvent-free processing route. Furthermore, ecological and economical aspects were considered by choosing cost-efficient, commercially available polymers. The collected data was evaluated regarding the structure-property relations of the studied three-component plastic crystal electrolytes (PCEs).

## EXPERIMENTAL SECTION

**Materials.** Succinonitrile (SN, ≥99%) was purchased from Sigma-Aldrich (Taufkirchen, Germany) or TCI Deutschland GmbH (Eschborn, Germany) and was used as received. Lithium bis(trifluoromethanesulfonyl)imide (LiTFSI, 99.9%) from IoLiTec GmbH (Heilbronn, Germany) was used as Li salt. The polymers polyacrylonitrile (N-PAN, $M_w$ = 80.000 g/mol) from Dolan GmbH (Kelheim, Germany) and poly(ethylene carbonate) (QPAC 25, $M_w$ = 50.000−200.000 g/mol) from Empower Materials (New Castle) were provided by named companies as a free sample. Poly(ethylene oxide) (PEO, $M_w$ = 100.000 g/mol) was supplied by Alfa Aesar and Thermo Fisher GmbH (Kandel, Germany), and poly(vinylpyrrolidone) (PVP, $M_w$ = 25.000 g/mol) by Merck Millipore (Darmstadt, Germany). Polymers were dried in vacuum for 24 h before use. A glass fiber nonwoven (30 g/m$^2$) was purchased from R&G (Waldenbuch, Germany) and was used as a separator.

**Physicochemical Properties of Selected Polymers.** Physicochemical properties of the selected polymers such as selected molar mass ($M$), morphology, calculated chain length, amount of the polymer ($N_{polymer}$), and the corresponding number of the polymer's repeating units ($N_{RU}$) in PCE + polymer are listed in Table 1.

**Preparation of Plastic Crystal Electrolyte (PCE) and Plastic Crystal Electrolyte with Polymer Additives (PCE + Polymer).** All preparation steps were carried out in an argon-filled glovebox (MBRAUN, $O_2$ and $H_2O$ <0.1 ppm). For a 0.4 mol/L mixture (PCE), SN was molten at 70 °C in a sand bath, and the corresponding amount of LiTFSI was added to the melt. The sample was stirred until a clear solution was obtained. For samples containing polymers (PCE + polymer), the same procedure was performed with the addition of 10% w/w of the appropriate polymers PEO, PVP, PEC, and PAN to the 0.4 mol/L LiTFSI-SN melt. The samples were stirred until homogeneous solutions were obtained.

**Characterization Methods.** Phase transitions of the PCE and the PCE + polymer and influences of thermal history on these phase transitions were examined by differential scanning calorimetry using a Discovery DSC (TA Instruments, Hüllhorst, Germany). LiTFSI-containing samples were weighed and sealed in hermetic aluminum pans under glovebox atmosphere. Heat flows of the samples were recorded upon heating and cooling in a temperature range between −80 and 100 °C in three distinct experiments. For the evaluation of thermal history influences, three different heating and cooling cycles were performed. The first experiment was performed with a heating ramp at 10 K/min and a cooling ramp at 5 K/min. Results from the second heating ramp were used for identification of characteristic phase transitions and comparison between the examined samples. Further experiments with a reduced cooling rate of 2 K/min (run 2, heating ramp at 10 K/min) or a reduced heating rate of 5 K/min (run 3, cooling ramp at 5 K/min) were conducted only for PCE + PEC and PCE + PAN.

Thermal and thermo-oxidative degradation of the PCE and the PCE + polymer was derived from mass loss, detected via thermogravimetric analysis with a Q5000 TGA (TA Instruments, Hüllhorst, Germany) under nitrogen atmosphere and air over a temperature range from 30 to 800 °C, respectively. The samples were weighed into platinum TGA crucibles under glovebox atmosphere and transferred into the instrument with minimal air exposure. A heating rate of 10 K/min was applied for all experiments.

Light microscopy was performed on a Keyence VHX-7000 digital microscope (Keyence Deutschland GmbH, Neu-Isenburg, Germany). Test samples were prepared in a glovebox by melting the regarding PCE and PCE-polymer samples and applying one droplet in the middle of a glass microscope slide. The applied drop was left at room temperature to cool down until solidification took place. For examination, the sample was


https://doi.org/10.1021/acsomega.2c02174
ACS Omega 2023, 8, 9058−9066

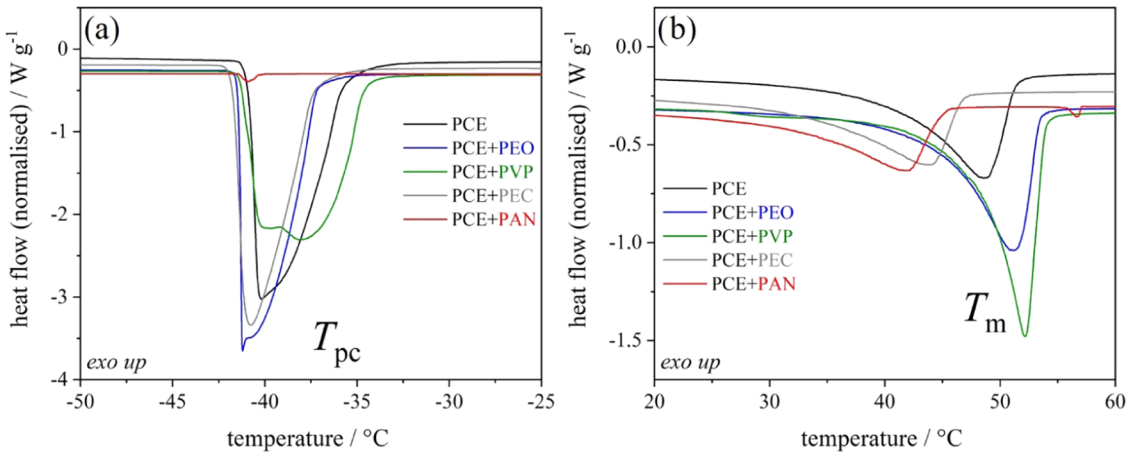


**Figure 1.** DSC thermograms of the second heating cycle with 10 K/min for the PCE and PCE + polymer showing (a) $T_{pc}$ range from −50 and −25 °C and (b) $T_m$ range from 20 to 60 °C.

**Table 2. Temperatures ($T_{pc}$, $T_m$) and Enthalpies ($\Delta H_{pc}$, $\Delta H_m$) for Solid Phase and Melting Transitions, as well as Calculated Rel. Crystallinity ($\chi_c$) of SN, Derived from DSC Experiments**

| | 2nd heating ramp | | | | | 3rd heating ramp | | | | |
|---|---|---|---|---|---|---|---|---|---|---|
| | $T_{pc}$, °C | $\Delta H_{pc}$, J/g | $T_m$, °C | $\Delta H_m$, J/g | $\chi_c$, % | $T_{pc}$, °C | $\Delta H_{pc}$, J/g | $T_m$, °C | $\Delta H_m$, J/g | $\chi_c$, % |
| Experiment 1: Heating 10 K/min and Cooling 5 K/min | | | | | | | | | | |
| PCE | −40.2 | 67.3 | 48.6 | 27.6 | 57.5 | −40.0 | 67.2 | 48.9 | 27.6 | 57.5 |
| PCE + PEO | −41.2 | 66.6 | 51.2 | 32.5 | 67.7 | −41.4 | 66.6 | 51.1 | 32.6 | 67.9 |
| PCE + PVP | −38.1 | 64.8 | 52.2 | 38.2 | 79.6 | −38.4 | 64.6 | 52.2 | 38.1 | 79.4 |
| PCE + PEC | −40.8 | 59.8 | 44.0 | 20.5 | 42.7 | none | none | 43.9 | 20.4 | 42.5 |
| PCE + PAN | −40.9 | 0.3 | 42.0 | 19.8 | 41.3 | −40.9 | 0.7 | 42.0 | 19.9 | 41.5 |
| Experiment 2: Heating 10 K/min and Cooling 2 K/min | | | | | | | | | | |
| PCE + PEC | −41.0 | 0.3 | 46.3 | 20.5 | 42.7 | none | none | 46.3 | 20.5 | 42.7 |
| PCE + PAN | none | none | 42.1 | 12.6 | 26.3 | none | none | 42.1 | 12.6 | 26.3 |
| Experiment 3: Heating 5 K/min and Cooling 5 K/min | | | | | | | | | | |
| PCE + PEC | −40.8 | 50 | 35.7 | 6.8 | 14.2 | −40.8 | 50.1 | 35.8 | 6.8 | 14.2 |
| PCE + PAN | −40.6 | 1.2 | 43.0 | 9.2 | 19.2 | −40.5 | 2 | 43.0 | 9.2 | 19.2 |

packed in a plastic box for transportation and examined quickly.

Rheological behavior upon cooling and heating was investigated via oscillation experiments with a Discovery Hybrid rheometer (TA Instruments, Hüllhorst, Germany) at a frequency of 1 Hz over a temperature range from 5 to 80 °C. Molten samples were loaded on the tempered base plate, and the loading gap between the parallel peltier steel plates was adjusted to 500 μm. Experiments were conducted with a constant strain of 40 1/rad (0.1%), in compliance with 1 mrad/N m. Heating and cooling rates were set at 1 K/min. Soak times for start temperatures were 120 s at 80 °C (cooling ramp) and 600 s at 5 °C (heating ramp).

All electrochemical experiments were conducted with an Interface 1010e potentiostat (Gamry Instruments, Warminster). For test cell assembling in EL-Cell test cells (ECC-Std, EL-Cell, Hamburg, Germany), samples were prepared by punching out a glass fiber nonwoven separator in a round shape of 18 mm diameter, which was infiltrated afterward with the melt of PCE or PCE + polymer, respectively. Glass fiber nonwoven was used because commercial separators like Celgard showed poor infiltration results.

For the investigation of ionic conductivity ($\sigma$), electrochemical impedance spectroscopy (EIS) was performed in a frequency range of $10^6$−1 Hz and an amplitude of 10 mV in a temperature range from 80 to −20 °C, using an Espec SU-242 temperature chamber (Espec Europe). The samples (infiltrated glass nonwoven) were sandwiched between two ion-blocking stainless steel electrodes of 50 μm thickness and 18 mm diameter. EIS measurements were proceeded every 10K, and cells were held at an appropriate temperature for 30 min prior to measurement for equilibration.

For electrochemical stability experiments, linear sweep voltammetry (LSV) was carried out on the samples. Stainless steel was used as the working electrode and lithium metal was chosen as the reference electrode. LSV was carried out at 50 °C in a voltage window from the open-circuit voltage (OCV) of the sample until 5.5 V vs lithium.

## RESULTS AND DISCUSSION

**Thermal Properties of PCE and PCE + Polymer Samples.** *Phase Transitions.* The solid−solid phase transitions and melting events of the PCE (SN containing 0.4 mol/L LiTFSI) and mixtures of PCE with the studied polymers PEO, PVP, PEC, and PAN (PCE + polymer) were determined by DSC experiments. In the second heating cycle, a first endothermic signal between −42 and −30 °C was observed in all samples, which was attributed to the solid−solid phase transition ($T_{pc}$) of SN from its crystalline to plastic crystalline state (Figure 1a). The corresponding peak maximum temperatures of PCE and PCE-polymer samples can be observed in



https://doi.org/10.1021/acsomega.2c02174
ACS Omega 2023, 8, 9058−9066

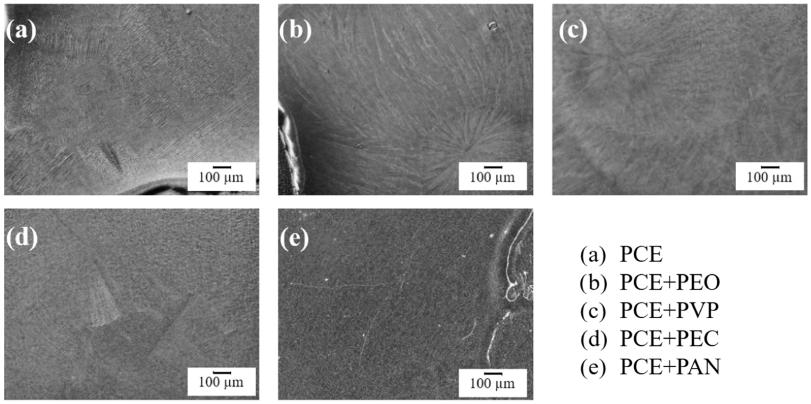


**Figure 2.** Light microscopy images of (a) PCE, (b) PCE + PEO, (c) PCE + PVP, (d) PCE + PEC, and (e) PCE + PAN.

the range of −42 and −38 °C and were used for comparison between the PCE and PCE + polymer.

In the absence of polymers, SN in the PCE exhibits a plastic crystalline transition enthalpy ($\Delta H_{pc}$) of $\Delta H_{pc}$ = 67.3 J/g and $T_{pc}$ = −40 °C, both remaining constant in the second and third heating cycle. The presence of the studied polymers PEO, PVP, PEC, and PAN in the corresponding PCE + polymer samples does not show a significant influence on $T_{pc}$. However, for PCE + PVP, the signal appears broader and bimodal, which indicates the presence of two different phases (Figure 1a). In contrast to PCE + PEO and PCE + PVP, $\Delta H_{pc}$ of SN in PCE + PEC diminished slightly to 59.8 J/g, whereas the plastic crystal phase transition was hardly detectable for PCE + PAN with $\Delta H_{pc}$ <1 J/g. In previous studies, a decrease of $\Delta H_{pc}$ of SN is often correlated to a higher disorder in the structure of SN.[9,13] This can be caused by an increase of *trans*-isomer concentration, which is mainly provoked by impurities like Li salt or polymers. From this, it can be assumed that SN in PCE + PAN is highly disordered, lacking a three-dimensional positional order. Furthermore, $T_{pc}$ disappeared completely in the third heating cycle for PCE + PEC, whereas $\Delta H_{pc}$ for PCE + PAN slightly increased from the second to the third heating cycle (Table 2, Experiment 1). This clearly points to a sensitivity of the crystallization processes in SN-rich electrolytes toward changes in temperature, time, and the polymeric additives. Several heating and cooling cycles may lead to structural reorganization that inhibits or facilitates crystallization processes.

With further temperature increase, melting ($T_m$, $\Delta H_m$) of SN in the PCE and the PCE + polymer is detected as a broad endothermic signal in the temperature range from 25 to 60 °C (Figure 1b), which is in agreement with the literature.[9,13,17] In comparison to polymer-free PCE ($T_m$ = 48.6 °C, $\Delta H_m$ = 27.6 J/g), the presence of polymers (PCE + polymer) influences the melting event slightly. For PCEs containing PEO or PVP, $T_m$ is shifted by 2−3 °C to higher temperatures and $\Delta H_m$ is increased to 38.2 J/g, in the case of PCE + PVP. In contrast, the presence of PEC or PAN lowers $T_m$ of SN in the PCEs to 42 and 44 °C, respectively, and decreases $\Delta H_m$ by 7−8 J/g. Since the polymers themselves do not show melting events below 60 °C, which could influence here discussed melting event, $\Delta H_m$, was used to evaluate the relative crystallinity ($\chi_c$) of SN in the PCE and in the PCE + polymer using eq 1) with $\Delta H_{m(SN)}$ = 48 J/g.[17]

$$\chi_c = (\Delta H_{m(\text{SN in PCE})} / \Delta H_{m(SN)}) \times 100\% \quad (1)$$

PCE + PEO and PCE + PVP reach the highest $\Delta H_m$ value among the studied PCEs with polymer with 32.5 and 38.1 J/g, respectively. The highest $\chi_c$ was calculated for PCE + PVP with $\chi_c$ = 80%. This higher degree of crystallinity is also identified by light microscopy, revealing crystalline lamelle-like superstructures (Figure 2c). For PCE + PEO, spherulite- and lamella-like structures can be explained by the semicrystalline nature of pristine PEO and interactions between the polymer's ether groups, SN and LiTFSI.[16,18] For a polymer electrolyte based on PVP and $LiClO_4$,[19] physical interactions between PVP and $LiClO_4$ ions were described to result in a complex network structure, increasing the overall crystallinity. The studied low-molecular-weight, amorphous PVP fraction (Table 1) showed an unexpected high influence on the PCE's morphology, which most probably results from appropriate intramolecular interactions between PVP and LiTFSI. The role of the polymer's functionality also becomes apparent by comparing PCEs containing PEC or PAN, which exhibit the lowest rel. crystallinity with $\chi_c$ = 43 and 41%, respectively. For PCE + PEC, a few crystalline domains can be identified and in the case of PCE + PAN, appropriate structures are missing in microscopy images (Figure 2d,e). Even though PAN is semicrystalline in its pristine form, the addition of Li salts has been reported to reduce the crystallinity in semicrystalline polymers.[5,6,20]

Additionally, a significant sensitivity of $T_{pc}$ and $T_m$ of PCE + PEC and PCE + PAN samples on heating and cooling rates was observed. For PCE + PAN, a reduction of the cooling rate from 5 to 2 K/min leads to an absence of SN's $T_{pc}$ in the second and third heating cycles with 10 K/min (Table 2, Experiment 2). For PCE + PEC, the reduced cooling rate of 2 K/min decreases $\Delta H_{pc}$ of SN upon the second heating cycle to only 0.3 J/g, and in the third heating cycle, the signal is not detectable. Increasing the heating and cooling rates to 5 K/min, respectively, yields an increase of $\Delta H_{pc}$ of SN in PCE + PAN to 1.2 J/g (second heating) and to 2 J/g (third heating), exceeding the ones from the first experiment with an accelerated cooling rate (Table 2, Experiment 3). The solid phase transition of SN in PCE + PEC reaches the highest $\Delta H_{pc}$ with 50 J/g in the third experiment, remaining constant in the examined heating cycles (Table 2, Experiment 3).

*Thermal and Thermo-Oxidative Degradation.* The influence of the polymers PEO, PVP, PEC, or PAN on the thermal and thermo-oxidative stability of the PCE was determined by thermogravimetric analysis (TGA) under nitrogen and air atmosphere.



https://doi.org/10.1021/acsomega.2c02174
ACS Omega 2023, 8, 9058−9066

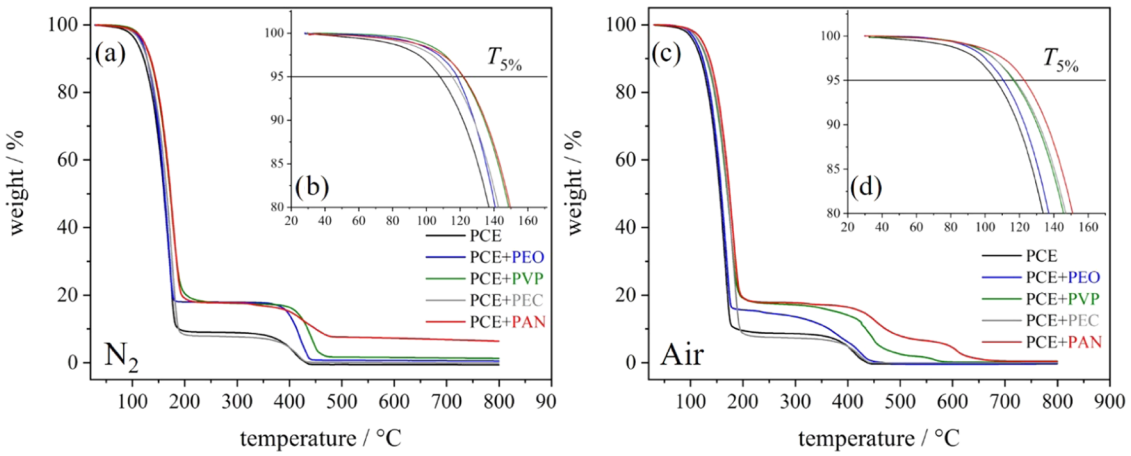


**Figure 3.** TGA ranging from 30 to 800 °C with a heating rate of 10 K/min for PCE and PCE + polymer samples under (a) nitrogen and (c) air atmosphere; (b, d) the area of $T_{5\%}$.

In a nitrogen atmosphere, two distinct mass loss events can be observed for all samples (Figure 3a). Up to 220 °C, PCEs containing PEO, PVP, or PAN show a mass loss of ∼80% of their initial weight. In agreement with the initial composition of PCE + polymer with 81.6% SN, 9.3% LiTFSI, and 9.1% polymer, this first mass loss can be attributed to the evaporation of SN. In contrast, PCE blended with PEC shows an increased weight loss of 92% until 220 °C. This can be explained by the simultaneous evaporation of SN and degradation of PEC, which exhibits a mass loss of 99% until 220 °C (Table S1). Thereof, the remaining 8% of the initial weight in PCE + PEC at $T$ > 220 °C can be related to the LiTFSI fraction, which degrades at temperatures above 300 °C (Table S1).

Moreover, the polymers' influence on the sublimation process of SN can be noticed and was determined with the onset temperature ($T_{onset}$) of the first mass loss step and the temperature at the initial mass loss of 5% ($T_{5\%}$) (Figure 3b). $T_{onset}$ indicates the beginning of the first mass loss step and was determined manually using tangents. For PCE, $T_{onset}$ for the first mass loss was determined at ∼40 °C. The presence of PEO or PVP in the PCE shifts $T_{onset}$ to higher temperatures, resulting in $T_{onset}$ ∼60 °C for both samples. In addition, PCE + PVP exhibits higher $T_{5\%}$ = 122 °C than the PCE without polymer ($T_{5\%}$ = 108 °C). An increase of $T_{onset}$ and $T_{5\%}$ could be an indicator for an inhibited sublimation process of SN due to the presence of polymers. One possible explanation for this could be the integration and trapping of SN in the polymer's structure. This could be especially the case for PCE + PEO and PCE + PVP, which cause the highest relative crystallinity of SN and corresponding crystalline structures (Table 2 and Figure 2). Entrapping due to polymer chain entanglement, as well as noncovalent interactions between the nitrile groups of SN and functional groups of the polymer, could further inhibit the sublimation of SN. However, it must be noted that melting events soften the PCEs, which could facilitate SN evaporation.

In comparison to PCEs containing PEO or PVP, the PCE + PEC and PCE + PAN reveal a $T_{onset}$ = 40−50 °C, which corresponds to the $T_{onset}$ of the PCE lacking polymer. As PCE + PEC and PCE + PAN also reveal melting events in the range of 42 and 44 °C, melting could facilitate the sublimation process. But, for PCE + PAN, the derived $T_{5\%}$ of 122 °C does not support this assumption.

A second mass loss step is observed for PCE samples in a temperature range from 330 to 500 °C. Since pristine SN shows a mass loss of 99% until 180 °C (Supporting Information), the observed mass loss step of PCE and PCE + polymer was aligned to the thermal degradation of LiTFSI and the appropriate polymers, respectively.

For a better comparison in this temperature region, the temperature at the inflection point ($T_{IP}$) of the identified mass loss step was determined at the peak maximum of the derivate mass loss. PCE + PVP exhibits the highest $T_{IP}$ with 444 °C, in comparison to the other PCE + polymer samples, showing $T_{IP}$ = 420 °C (Table S2). Also, in comparison with pristine PVP, exhibiting $T_{IP}$ = 434 °C (Table S1), PCE + PVP demonstrates an enhanced thermal stability. It is assumed that noncovalent interactions between PVP and LiTFSI, as described for a PVP-$LiClO_4$,[19,21] could create complex network structures resulting in an increased thermal stability. At 800 °C, all samples reach a residual mass of <1%, with exception of PCE blended with PVP or PAN with a residue of 1.3 and 6.4%, respectively, being more prone to char formation.

In air atmosphere, PCE samples reveal almost the same behavior until 220 °C as observed in a $N_2$ atmosphere. However, in comparison to a $N_2$ atmosphere, PCE + polymer samples show a deviant behavior in the temperature range between 220 and 650 °C attributed to thermo-oxidative degradation mechanisms. As the PEC degrades completely until 220 °C, a polymer impact at $T$ > 220 °C can be ruled out, and the observed mass loss of PCE + PEC with $T_{IP}$ = 420 °C is solely related to LiTFSI degradation. In contrast, PCE + PVP and PCE + PAN show two overlapping mass loss steps (Figure 3c) at temperatures above 300 °C. For the first partial mass loss, $T_{IP}$ corresponds to ∼450 °C for both samples. In the second step, PCE + PAN shows a higher $T_{IP}$ at 607 °C (Table S2) than PCE + PVP with $T_{IP}$ = 566 °C. It can be assumed that within the first mass loss step, LiTFSI degrades, which corresponds to $T_{IP}$ of 420 °C for pristine LiTFSI. The second mass loss can be related to thermo-oxidative degradation reactions of PVP and PAN.

At 800 °C in air atmosphere, all samples exhibit a residual mass <1% of the initial weight, indicating a complete degradation under air atmosphere.

**Thermomechanical Properties of the PCE.** Thermomechanical properties of the PCE and PCE + polymer samples were studied by oscillation experiments with a rheometer at 1



https://doi.org/10.1021/acsomega.2c02174
ACS Omega 2023, 8, 9058−9066

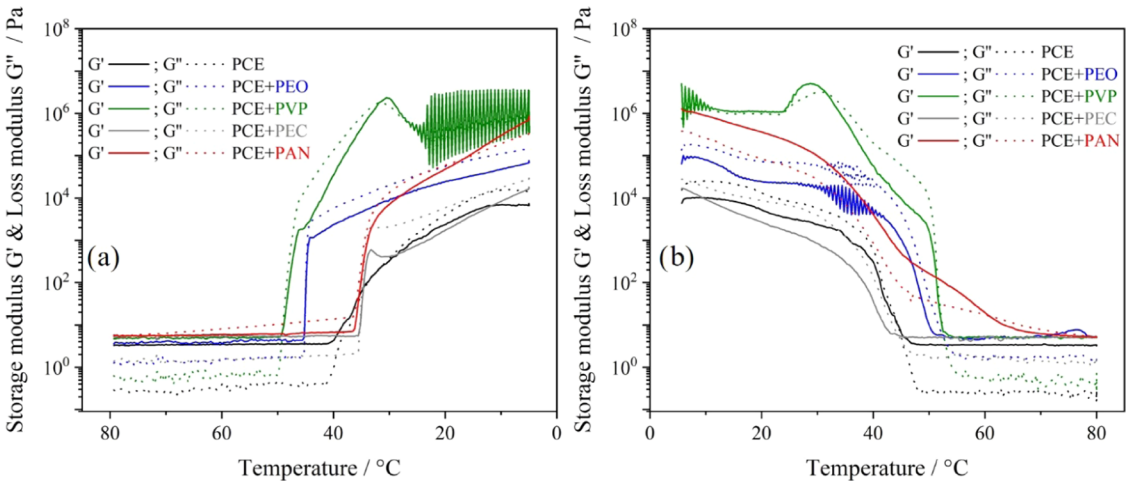


**Figure 4.** Development of storage modulus ($G'$) and loss modulus ($G''$) over temperature for the PCE and PCE + polymer upon (a) cooling and (b) heating.

Hz in cooling and heating cycles. Here, the magnitudes of storage modulus ($G'$) and loss modulus ($G''$) of the respective PCEs demonstrate a certain dependence on the added polymer and applied temperature. For all samples, two distinct areas upon cooling and heating can be noted, which are related to the PCE's response in its liquid or solid, plastic crystalline state.

In the cooling cycle, starting from melt at 70 °C, the PCE exhibits $G'$ = 3.3 Pa and $G''$ = 0.3 Pa. With $G'$ exceeding $G''$, a tan $\delta$ of 0.1 (tan $\delta = G''/G'$) results, indicating a higher amount of the elastic components than the viscous component (Figure 4a). This result is surprising, expecting a melted system at 70 °C. At the same temperature, the presence of the polymers PEO, PVP, or PEC in the PCE increases slightly both moduli, compared to the PCE without polymer, whereby tan $\delta$ remains <1 for these samples. In comparison, PCE + PAN shows the highest moduli with $G'$ = 5.5 Pa and $G''$ = 6.3 Pa and a deviant tan $\delta$ with 1.1. These results lead to the conclusion that PCE + PAN contains more elastic components in melt than the other examined PCE + polymer samples.

In a temperature area from 50 to 35 °C, a sharp increase of the moduli by a factor of 1000 is observed for all samples. This increase is related to the phase transition from the liquid to solid phase as mentioned in the discussion of DSC experiments (Figure 4a). The characteristic temperature for this phase transition, $T_{\delta_{max}}$, was derived from the peak maximum of tan $\delta$ (Figure S2). The PCE without polymer exhibits a $T_{\delta_{max}}$ at 36.2 °C. As expected, from the observed polymer influences on melting events ($T_m$) in DSC experiments, the presence of PEO and PVP also shifts $T_{\delta_{max}}$ to higher temperatures with $T_{\delta_{max}}$ = 44 °C. In contrast, the presence of PEC and PAN in the PCE reduces $T_{\delta_{max}}$ to 29.2 and 35.2 °C, respectively. Since the discussed $T_{\delta_{max}}$ was recorded upon cooling and $T_m$ was detected upon heating, this certain discrepancy between those two data points was expected.

For all samples, both moduli increase with decreasing temperature, whereas $G''$ always exceeds $G'$ resulting tan $\delta$ > 1. Thus, despite solidification, the viscous component governs the viscoelastic solids. At 20 °C, the PCE without polymer reaches moduli of $G'$ = 0.2 kPa and $G''$ = 0.4 kPa. The presence of PEO in the PCE increases $G'$ to 2.3 kPa and $G''$ to 5.5 kPa. The evaluation of $G'$ and $G''$ at $T$ < 30 °C for PCE + PVP was not possible due to rattling effects (Figure 4). However, in the temperature range from 50 to 30 °C, PCE + PVP exhibits the most pronounced increase of both moduli, exceeding the ones detected for PCE + PEO. Comparing the here examined polymer additives PEO and PVP, PVP has a lower molecular weight and chain length than PEO. Thereof, earlier drawn correlation to a determining factor of the polymers functional groups on the resulting properties of the PCE + polymer could also apply here. In comparison, PCE + PEC exhibits the lowest moduli with $G'$ = 0.1 kPa and $G''$ = 0.6 kPa. Further, the presence of the here examined PEC in the PCE increases the viscous component in the PCE while lowering the amount of elastic components.

After sample equilibration at 5 °C for 600 s, the heating cycle followed. For the PCE and PCE + polymer with PEO, PVP, or PEC, the observations are similar to the ones observed in the cooling cycle. PCE + PAN shows deviant behavior upon heating, with $G'$ exceeding $G''$ below 64 °C, and above $T_{\delta_{max}}$, the other way around ($G' < G''$) (Figure 4b). Thus, below $T_{\delta_{max}}$, in its solid, plastic crystalline phase, elastic components appear to determine the viscoelastic properties of PCE−PAN. The differences between the sample's response upon cooling or heating can be explained by deviating kinetics regarding the crystallization/solidification or melting process. As observed in DSC experiments, phase transitions in the PCE + PAN showed a high dependency on the chosen heating and cooling rates. This may also have an effect on the rheological response with set heating and cooling rates. In addition, influences of mechanical stress, here, namely, frequency, can also intervene in crystallization processes and is yet to be fully understood.

**Electrochemical Properties.** *Ionic Conductivity.* Exemplary Nyquist plots from EIS measurements, depicted in Figure 5, exhibit a high-frequency semicircle and low-frequency straight line representing typical elements of a polymer electrolyte placed between ion-blocking stainless steel electrodes.[22] The semicircle is attributed to the resistive and capacitive properties of samples' bulk, while the straight line is the result of the capacitive properties of the ion-blocking stainless steel electrodes. To determine the resistance of the PCE samples, the $Z_{real}$ value at the high frequency end of the


https://doi.org/10.1021/acsomega.2c02174
ACS Omega 2023, 8, 9058−9066

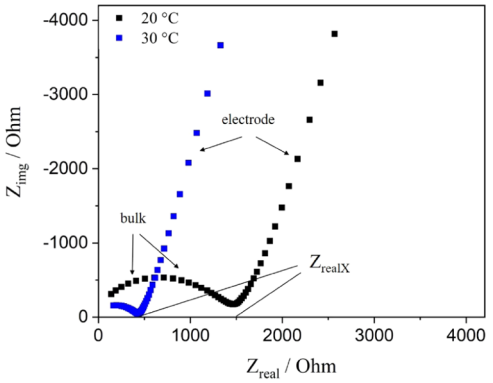


**Figure 5.** Exemplary Nyquist plots of a representative PCE sample (0.4 M LiTFSI-SN) at 30 and 20 °C.

straight line ($Z_{realX}$) was used as the resistance value to calculate ionic conductivities.

The ionic conductivity is calculated using eq 2) with a sample radius $r$ = 0.9 cm, the sample thickness $d$, and corresponding $Z_{real\,X}$ for each sample and temperature.

$$\sigma = \frac{d}{\pi \cdot r^2} \cdot Z_{real\,X} \tag{2}$$

The derived ionic conductivities of the PCE and the PCE + polymer are displayed in Figure 6 as an Arrhenius type.

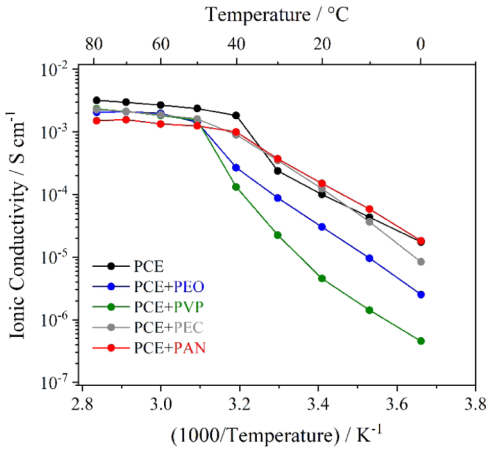


**Figure 6.** Arrhenius plot of ionic conductivities between 0 and 80 °C for the PCE and PCE + polymer.

For all samples, two areas with an explicit curve development can be observed from 80 to 40 °C (first area) and from 40 to 0 °C (second area). In the first area, $\sigma$ reaches values up to $10^{-3}$ S/cm for all samples. In this temperature region, the samples are expected to be molten. In melt, the PCE without polymer exhibits the highest values for $\sigma$ and the addition of here examined polymers decreases $\sigma$ slightly. As described for polymer electrolyte melts, the ion mobility is correlated to numerous factors like the diffusion coefficient. Assigned to here studied PCE + polymer samples, diffusion coefficients are unknown, and thereof, no correlations between the chosen polymers with resulting $\sigma$ values of the corresponding PCE + polymer melt will be drawn at this point.

In the second temperature area, from 40 to 0 °C, $\sigma$ decreases with decreasing temperature and a pronounced influence of the polymer can be observed (Figure 6). At 20 °C, the PCE without polymer exhibits $\sigma$ = 1.0 × $10^{-4}$ S/cm, which is in good agreement with the literature values for SN doped with Li salts.[10,13] Hence, the effect of the used glass fiber nonwoven separator on conductivity is negligible at this point. At 20 °C, the presence of PEO or PVP in the PCE reduces $\sigma$ to 3.0 × $10^{-5}$ and 4.6 × $10^{-6}$ S/cm, respectively. In contrast, $\sigma$ slightly increases in the presence of PEC and PAN to 1.2 × $10^{-4}$ and 1.5 × $10^{-4}$ S/cm, respectively. Here, correlations with earlier discussed observations of the polymers influence on the PCEs' morphology could also apply. For example, at 20 °C, $\sigma$ decreases with increasing crystallinity of SN in the PCE + polymer. PCE + PAN, described as completely amorphous, exhibits the highest values for $\sigma$ at $T$ = 20 °C. As described for polymer electrolytes, a beneficial effect of amorphous disorder in the PCE + polymer samples on the ionic conductivity can be observed in this study.

Comparing PCEs containing PEO or PVP, influences of the polymer's functional groups on the ionic conductivity can be further discussed. As mentioned, PVP is amorphous with a small chain length, whereof it is expected to facilitate ion mobility, whereas the semicrystalline nature of PEO and longer polymer chains were expected to inhibit ion mobility. But, it appears that physical interactions/complexation of PVP's functional groups with LiTFSI and SN, as mentioned earlier, have a stronger inhibiting effect on the ion mobility than comparable interactions/complexation with PEO. Also, $\sigma$ for PCE + PVP could be decreased due to immobile $TFSI^-$ counterions, which coordinate to PVP's amid groups.

The activation energy ($E_A$) for Li-ion migration in PCEs in the plastic crystalline phase ($T$ < 40 °C, melting DSC) was determined with the slope of regarding Arrhenius diagrams. For the PCE without polymer, $E_A$ reaches 0.7 eV (Table 3).

**Table 3. From Arrhenius Diagrams Derived Values of $E_A$ in the Plastic Crystalline Phase ($T$ < 40 °C) of Examined PCE and PCE + Polymer Samples**

| sample | $E_A$ (EIS), eV |
|---|---|
| PCE | 0.7 |
| PCE + PEO | 0.85 |
| PCE + PVP | 1.15 |
| PCE + PEC | 0.85 |
| PCE + PAN | 0.72 |

The presence of the here used polymer additives increases $E_A$, with the exception of PAN. The increase of $E_A$ can have various reasons like sterical hindrance due to the polymer chain entanglement or strong interactions between functional groups of the polymer and Li-ions. Strong physical interactions between LiTFSI ions and PVP, as discussed earlier, can be the reason for PCE + PVP, showing the highest $E_A$ = 1.15 eV in this study. In addition, the possible network structure in PCE + PVP can act as a sterical hindrance for ion migration. PCE + PAN showing the lowest $E_A$ = 0.72 eV within the PCE + polymer comparison, indicating a less energy consuming migration of Li-ions. It can be assumed that the amorphous structure of PCE + PAN (Figure 2) compared to other PCE + polymer samples also reduces $E_A$. However, the underlying mechanism of ion transfer in the plastic crystalline state of an SN-based electrolyte doped with polymer additives is not fully understood yet.[23]

*Electrochemical Stability Window.* The oxidative limit of the electrochemical stability window at room temperature was


https://doi.org/10.1021/acsomega.2c02174
ACS Omega 2023, 8, 9058−9066

determined via linear sweep voltammetry (LSV) for the PCE and PCE + polymer samples infiltrated in glass fiber nonwoven. The stability window was determined by the maximum voltage vs reference (lithium metal) before a significant increase in current is overserved (Figure 7).

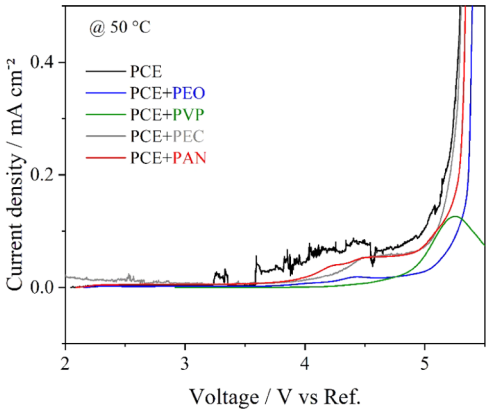


**Figure 7.** Voltamogram of the PCE and PCE + polymer from LSV experiments with a scan rate of 1 mV/s at 50 °C.

Measurements were carried out at 50 °C for all samples to ensure comparable conductivity values of all samples. For the PCE without polymer, the current does not increase significantly until 5 V, indicating SN in the PCE as electrochemically stable up to 5 V vs lithium in the chosen setup. This is in accordance with previously reported observations.[10] However, the current density at lower voltages heavily fluctuates. This might be due to chemical instabilities of succinonitrile in contact with lithium metal. The addition of polymers smoothens the current density curve and slightly increases the electrochemical stability window. The results indicate a reasonable stability for possible application in batteries. Although, for specific cathode materials, stability needs to be checked, since introducing reactive materials, such as cathode active materials, may lead to results different from inert stainless steel electrodes used here.

For PCEs with PEO, PEC, and PAN, a slight increase in current, starting at 4.0 V, and a drastic increase in current, starting at 4.9 V, is detected. Since the minor increase in current is independent of the chosen polymer, it could be a reaction of the chosen lithium salt LiTFSI, as described previously.[24] Furthermore, a decomposition of PEC at >4.5 V has been reported.[25] Nevertheless, the authors concluded a suitability for PEC electrolytes for application. For PVP, the overall lower current densities are recorded although the temperature was increased to 50 °C to ensure comparable ionic conductivity. Furthermore, PVP exhibits a peak in current density at 5.25 V, which indicates a redox reaction taking place. To further analyze this phenomenon, cyclic voltammetry experiments are necessary, which is beyond the scope of this publication.

## CONCLUSIONS

We have demonstrated that the presence of the polymers PEO, PVP, PEC, and PAN influences the thermomechanical and electrochemical properties of an SN-based plastic crystalline electrolyte (PCE). While the plastic crystalline phase transition event of SN was not affected significantly, PEO and PVP increased the melting temperature of SN in the PCE. Above this, the highest relative crystallinity of SN of 80% was observed for PCE + PVP, leading to microscopic lamelle-like superstructures due to additional physical interactions between the polymer functional groups and the remaining components.

Regarding the thermal stability, the presence of polymers proved to delay SN sublimation, most likely due to entrapping of SN in the polymer chain entanglements, crystalline structures, and by noncovalent interactions. In contrast to PCE ($T_{5\%}$ = 107 °C), PCE + PVP and PCE + PAN showed the strongest effect on the sublimation of SN with $T_{5\%}$ shifted to 122 °C. In agreement with the phase transition events, all polymers increased storage and loss moduli of the SN-based PCE above the melting temperature except for PEC. Electronic effects between PEC and SN seem to suppress the plastic crystalline state of SN diminishing thermomechanical stability. For all PCE + polymer, the viscous components exceeded the viscoelastic material properties, whereas PCE + PAN showed exceptional behavior with solid components determining the viscoelastic properties of PCE + PAN below $T_{\delta_{max}}$.

The ionic conductivity of the here examined SN-based electrolyte is reduced by polymers PEO or PVP, whereby the addition of PEC or PAN slightly increases the conductivity at room temperature.

This shows that all properties of an SN-based electrolyte can be tailored and improved by a polymer additive. In sum, the addition of PAN to the SN-based electrolyte shows a synergetic effect on mechanical and electrochemical properties, increasing both storage and loss moduli as well as ionic conductivity.

## ASSOCIATED CONTENT

### Supporting Information

The Supporting Information is available free of charge at https://pubs.acs.org/doi/10.1021/acsomega.2c02174.

Additional analysis data for thermal and mechanical characterization, including TGA results of raw materials (PDF)

## AUTHOR INFORMATION

### Corresponding Author

**Katharina Koschek** − *Adhesive Bonding Technology and Surfaces, Fraunhofer Institute for Manufacturing Technology and Advanced Materials (IFAM), 28359 Bremen, Germany; Department of Biology/Chemistry, University of Bremen, 28359 Bremen, Germany;* orcid.org/0000-0001-7398-3528; Email: Katharina.Koschek@ifam.fraunhofer.de

### Authors

**Vanessa van Laack** − *Adhesive Bonding Technology and Surfaces, Fraunhofer Institute for Manufacturing Technology and Advanced Materials (IFAM), 28359 Bremen, Germany; Department of Biology/Chemistry, University of Bremen, 28359 Bremen, Germany;* Present Address: Kleine Jüch 26, 50374 Erftstadt, Germany

**Frederieke Langer** − *Electrical Energy Storage, Fraunhofer Institute for Manufacturing Technology and Advanced Materials (IFAM), 38108 Braunschweig, Germany;* orcid.org/0000-0003-3099-0722

**Andreas Hartwig** − *Adhesive Bonding Technology and Surfaces, Fraunhofer Institute for Manufacturing Technology and Advanced Materials (IFAM), 28359 Bremen, Germany; Department of Biology/Chemistry, University of Bremen,*



https://doi.org/10.1021/acsomega.2c02174
ACS Omega 2023, 8, 9058−9066

*28359 Bremen, Germany;* orcid.org/0000-0002-3320-6414

Complete contact information is available at: https://pubs.acs.org/10.1021/acsomega.2c02174

### Author Contributions

This manuscript was written through contributions of all authors. All authors have given approval to the final version of the manuscript.

### Funding

This work was supported by the Fraunhofer Internal Programs MAVO under Grant No. 836 915 referring to the project "KOBIBATT".

### Notes

The authors declare no competing financial interest.

## ■ ACKNOWLEDGMENTS

The authors would like to thank Dolan GmBH and Empower Materials providing free polymer samples for this research. Further, the authors thank their colleagues Iris Gottschalk and Kerstin Flothmeier for performing DSC, TGA, and rheology experiments and the discussion of results.

## ■ ABBREVIATIONS

SN, succinonitrile; LiTFSI, lithium bis-(trifluoromethansulfonyl)imide; PEO, poly(ethylene oxide); PVP, poly(vinylpyrrolidone); PEC, poly(ethylene carbonate); PAN, polyacrylonitrile; PCE, plastic crystalline electrolyte; DSC, differential scanning calorimetry; TGA, thermogravimetric analysis; EIS, electrochemical impedance spectroscopy; LSV, linear sweep voltammetry; OCV, open-circuit voltage

## ■ REFERENCES

(1) Taib, N. U.; Idris, N. H. Plastic crystal−solid biopolymer electrolytes for rechargeable lithium batteries. *J. Membr. Sci.* **2014**, *468*, 149−154.
(2) Kim, G.-Y.; Petibon, R.; Dahn, J. R. Effects of Succinonitrile (SN) as an Electrolyte Additive on the Impedance of LiCoO 2 /Graphite Pouch Cells during Cycling. *J. Electrochem. Soc.* **2014**, *161*, A506−A512.
(3) Abouimrane, A.; Davidson, I. J. Solid Electrolyte Based on Succinonitrile and LiBOB. *J. Electrochem. Soc.* **2007**, *154*, A1031.
(4) Fergus, J. W. Ceramic and polymeric solid electrolytes for lithium-ion batteries. *J. Power Sources* **2010**, *195*, 4554−4569.
(5) Mindemark, J.; Lacey, M. J.; Bowden, T.; Brandell, D. Beyond PEO—Alternative host materials for Li + -conducting solid polymer electrolytes. *Prog. Polym. Sci.* **2018**, *81*, 114−143.
(6) Sun, C.; Liu, J.; Gong, Y.; Wilkinson, D. P.; Zhang, J. Recent advances in all-solid-state rechargeable lithium batteries. *Nano Energy* **2017**, *33*, 363−386.
(7) Yue, L.; Ma, J.; Zhang, J.; Zhao, J.; Dong, S.; Liu, Z.; Cui, G.; Chen, L. All solid-state polymer electrolytes for high-performance lithium ion batteries. *Energy Storage Mater.* **2016**, *5*, 139−164.
(8) Abouimrane, A.; Whitfield, P. S.; Niketic, S.; Davidson, I. J. Investigation of Li salt doped succinonitrile as potential solid electrolytes for lithium batteries. *J. Power Sources* **2007**, *174*, 883−888.
(9) Derollez, P.; Lefebvre, J.; Descamps, M.; Press, W.; Fontaine, H. Structure of succinonitrile in its plastic phase. *J. Phys.: Condens. Matter* **1990**, *2*, 6893−6903.
(10) Patel, M.; Bhattacharyya, A. J. Plastic−polymer composite electrolytes: Novel soft matter electrolytes for rechargeable lithium batteries. *Electrochem. Commun.* **2008**, *10*, 1912−1915.
(11) Fan, L.-Z.; Wang, X.-L.; Long, F.; Wang, X. Enhanced ionic conductivities in composite polymer electrolytes by using succinonitrile as a plasticizer. *Solid State Ionics* **2008**, *179*, 1772−1775.
(12) Fan, L.-Z.; Hu, Y.-S.; Bhattacharyya, A. J.; Maier, J. Succinonitrile as a Versatile Additive for Polymer Electrolytes. *Adv. Funct. Mater.* **2007**, *17*, 2800−2807.
(13) Alarco, P.-J.; Abu-Lebdeh, Y.; Abouimrane, A.; Armand, M. The plastic-crystalline phase of succinonitrile as a universal matrix for solid-state ionic conductors. *Nat. Mater.* **2004**, *3*, 476−481.
(14) Yue, R.; Niu, Y.; Wang, Z.; Douglas, J. F.; Zhu, X.; Chen, E. Suppression of crystallization in a plastic crystal electrolyte (SN/LiClO4) by a polymeric additive (polyethylene oxide) for battery applications. *Polymer* **2009**, *50*, 1288−1296.
(15) Coeler, M.; van Laack, V.; Langer, F.; Potthoff, A.; Höhn, S.; Reuber, S.; Koschek, K.; Wolter, M. Infiltrated and Isostatic Laminated NCM and LTO Electrodes with Plastic Crystal Electrolyte Based on Succinonitrile for Lithium-Ion Solid State Batteries. *Batteries* **2021**, *7*, 11.
(16) Gupta, R. K.; Kim, H.-M.; Rhee, H.-W. Poly(ethylene oxide): succinonitrile—a polymeric matrix for fast-ion conducting redox-couple solid electrolytes. *J. Phys. D: Appl. Phys.* **2011**, *44*, 205106.
(17) Acree, W. E. Thermodynamic properties of organic compounds: enthalpy of fusion and melting point temperature compilation. *Thermochim. Acta* **1991**, *189*, 37−56.
(18) Gupta, R. K.; Rhee, H.-W. A Detailed Investigation into the Electrical Conductivity and Structural Properties of [Poly(ethylene oxide)-succinonitrile]-Li(CF 3 SO 2) 2 N Solid Polymer Electrolytes. *Bull. Korean Chem. Soc.* **2017**, *38*, 356−363.
(19) Wu, H.-D.; Wu, I.-D.; Chang, F.-C. The interaction behavior of polymer electrolytes composed of poly(vinyl pyrrolidone) and lithium perchlorate (LiClO4). *Polymer* **2001**, *42*, 555−562.
(20) Long, L.; Wang, S.; Xiao, M.; Meng, Y. Polymer electrolytes for lithium polymer batteries. *J. Mater. Chem. A* **2016**, *4*, 10038−10069.
(21) Chen, R.; Liu, F.; Chen, Y.; Ye, Y.; Huang, Y.; Wu, F.; Li, L. An investigation of functionalized electrolyte using succinonitrile additive for high voltage lithium-ion batteries. *J. Power Sources* **2016**, *306*, 70−77.
(22) Langer, F.; Bardenhagen, I.; Glenneberg, J.; Kun, R. Microstructure and temperature dependent lithium ion transport of ceramic−polymer composite electrolyte for solid-state lithium ion batteries based on garnet-type Li7La3Zr2O12. *Solid State Ionics* **2016**, *291*, 8−13.
(23) Voigt, N.; van Wüllen, L. The effect of plastic-crystalline succinonitrile on the electrolyte system PEO:LiBF4: Insights from solid state NMR. *Solid State Ionics* **2014**, *260*, 65−75.
(24) Zainuddin, Z.; Hambali, D.; Supa'at, I.; Osman, Z. Ionic conductivity, ionic transport and electrochemical characterizations of plastic crystal polymer electrolytes. *Ionics* **2017**, *23*, 265−273.
(25) Okumura, T.; Nishimura, S. Lithium ion conductive properties of aliphatic polycarbonate. *Solid State Ionics* **2014**, *267*, 68−73.